DOWN-REGULATION OF L-TYPE CA^{2+} CURRENT IN LEFT ATRIAL MYOCYTES OF RATS DURING EXPERIMENTAL CARDIAC HYPERTROPHY

Chunpeng Zhang[1], Yosuke Okamoto[2], Takayoshi Ohba[2], Kazuyuki Ishibashi[1], Hiroshi Yamamoto[1], Kyoichi Ono[2] and Fumio Yamamoto[1]

(received 14 December 2012, accepted 26 December 2012)

[1]Department of Cardiovascular surgery, Akita University Graduate School of Medicine, Akita, Japan
[2]Department of Cell Physiology, Akita University Graduate School of Medicine, Akita, Japan

Abstract

Background : Cardiac hypertrophy is often associated with atrial arrhythmias, but there are limited experimental reports on small animal models of hypertrophied atria. Transverse aortic constriction (TAC) is an established model for ventricular hypertrophy and causes atrial hypertrophy and arrhythmias.

Purpose : We aim to investigate the atrial remodeling caused by an experimental model of elevated afterload in rats.

Methods and results : Eight weeks after creating TAC, hemodynamic, histological, and electrophysiological analyses were carried out in 8 week old rats. Sham operated rats were included as controls. The whole-cell patch-clamp technique was used to record action potentials (APs) and L-type Ca^{2+} current in isolated atrial myocytes. TAC resulted in hypertrophy in atrial and ventricular cardiomyocytes, accompanied by shortening of the atrial effective refractory period and an increase in atrial fibrillation (AF) inducibility by rapid atrial pacing. Atrial hypertrophy was associated with a shortening of AP duration and a decrease in L-type Ca^{2+} channel current density. Cav1.2 subunit mRNA expression was significantly reduced ($p<0.05$), which was paralleled by a significant increase in ANF and BNP expression in the TAC group compared with that in the sham group ($p<0.05$).

Conclusions : TAC causes left atrial hypertrophy, associated with alteration of electrophysiological and molecular properties of L-type Ca^{2+} channels.

Key words : L-type Ca^{2+} current, cardiac hypertrophy, atrial fibrillation, atrial myocytes

Introduction

Atrial fibrillation (AF) is the most common sustained cardiac arrhythmia, and contributes to hospitalization, morbidity, and mortality in the general population[1]. AF often coexists with several cardiovascular disorders in many patients, such as ischemic heart disease, cardiomyopathy, valvular disease, and hypertension[2]. The prevalence of AF in patients with left ventricular hypertrophy and failure is estimated to be 15-30%, which is approximately 10-fold higher than that in the general population[3]. Although cardiac hypertrophy may be compensatory enlargement of the heart aimed at reducing stress induced by pressure-volume overload[4], hemodynamically overloaded ventricles and/or atria are subject to cellular structural and electrical remodeling[5], which leads to the

Correspondce : Fumio Yamamoto, M.D.
Department of Cardiovascular Surgery, Akita University Graduate School of Medicine, 1-1-1, Hondo, Akita 010-8543, Japan
Tel : 81-18-884-6135
Fax : 81-18-836-2625
E-mail : f-yama@cvs.med.akita-u.ac.jp

occurrence of arrhythmias, including AF[6].

A possible change in L-type Ca^{2+} channel current (I_{CaL}) is considered an important factor in electrical remodeling of cardiac myocytes in AF or in dilated atria, contributing to the shortening of the action potential (AP), the refractory period, or the formation of reentrant circuits[7]. In contrast to tachycardia-induced ionic remodeling, however, several clinical and experimental studies have indicated a decrease, no change, or even an increase in I_{CaL} density in chronic heart failure, depending on the experimental conditions[8]. To better understand AF pathophysiology in conjunction with hypertrophied atria, multiple animal models have been developed. In particular, recent studies have reported small animal models of AF and/or hemodynamically overloaded atria. These models include rapid transesophageal atrial pacing in mice or rats[9,10], abdominal aortocaval shunts in the rat[11], chronic treatment of rats with angiotensin II[12], Zucker obese rats[13], monocrotaline-treated rats[14], and spontaneously hypertensive rats[15]. These are commonly accepted as useful models, because most animal models increase the inducibility of AF in response to rapid atrial pacing. However, electrophysiological properties of isolated atrial myocytes have not yet been fully analyzed. In the present study, chronic ventricular and atrial hypertrophy was induced by transverse aortic constriction (TAC) in rats, and hypertrophy-induced changes in I_{CaL} of left atrial (LA) myocytes and their potential contribution to arrhythmogenesis were investigated.

Methods

Experimental Animals

The protocols used in this study were approved by The Animal Ethics Committee of Akita University School of Medicine. Pressure overload was induced in isoflurane-anesthetized Wistar rats (aged 8 weeks) through TAC. After anesthesia was induced and maintained by spontaneous inhalation with 2-5% isoflurane, the transverse aorta was accessed through the second left intercostal space. A titanium clip was placed around the aortic arch between the brachiocephalic and left common carotid arteries, creating TAC. In sham operations, the procedure was identical, except constriction of the aortic arch was not performed. The rats were then allowed to recover and returned to their cages. All animals were maintained on a 12 : 12-h light-dark cycle for 8 weeks, while allowed free access to food and water, and they were then used for the experiments described below.

Echocardiographic Recording, Measurement of Hemodynamic Parameters, and Electrophysiological Studies (EPSs)

The TAC- and sham-operated rats were anesthetized by spontaneous inhalation with 2-5% isoflurane. Under spontaneous respiration, 2-dimensional transthoracic echocardiography with a 12-MHz probe was performed. Parasternal short-axis views were recorded at the level of the papillary muscles. The left ventricular end-diastolic dimension and end-systolic dimension were recorded. Ejection fraction was calculated by the Teicholz method. The blood pressure of bilateral carotid arteries was also recorded using a pressure transducer connected to a monitor (DynaScope 5100E ; Fukuda Denshi, Tokyo, Japan). A right cervical vein cutdown was then performed and a 2-Fr quadripolar electrode catheter with a 2-mm electrode distance (Ensemble ; Japan Lifeline, Tokyo, Japan) was inserted into the coronary sinus to perform the EPS. The tip of the catheter was placed at the site where the amplitude of the atrial wave was higher than that of the ventricular wave. A surface electrocardiogram (lead II) was also recorded. To measure the atrial muscle effective refractory period (AERP), a programmable stimulator (SEN-7203 ; Nihon Kohden, Tokyo, Japan) was used to deliver approximately twice the threshold current with a 2-ms duration. The AERP was measured at basic cycle lengths of 150 ms, 120 ms, and 100 ms. A train of 8 basic stimuli was followed by a single extra-stimuli with various intervals. The interval was decreased in steps of 5 ms, and AERP was defined as the longest interval that failed to capture the atrial wave. To induce AF, atrial burst pacing was delivered through 2 poles on the electrode catheter by a programmable stimulator at an amplitude of 6 volts, a cycle length of 20 ms, a pulse duration of 6 ms, and a stimulation time of 30 s. AF inducibility was determined by calculating the number of AF episodes divided by the number of total procedures. The AF duration

was defined as the interval between initiation and spontaneous termination of AF.

Histological Study

Tissue samples from the left atrium (LA) and left ventricle were fixed with 4% paraformaldehyde, embedded in paraffin, and sliced into 5-μm-thick sections. Sections were stained with hematoxylin/eosin and Masson's trichrome. To quantitatively evaluate cell size, the cross-sectional area of LA myocytes was measured from a tissue section of the hearts in the TAC and sham groups using confocal microscopy. In each field, the cross-sectional area of all transversally cut myocytes showing a nucleus was measured (LSM Image Browser, Zeiss, Germany). At least 50 myocytes in each region were measured.

Cell isolation

Single LA myocytes were isolated from rat hearts using protocols as described previously[14]. Briefly, hearts were rapidly excised and perfused at 37°C via the coronary arteries with oxygenated normal Tyrode's solution, followed by a 5-min perfusion with a Ca^{2+}-free Tyrode's solution. Hearts were then perfused with Ca^{2+}-free Tyrode's solution containing 0.05% collagenase (Wako Pure Chemicals, Osaka, Japan) and 0.005% elastase (Wako Pure Chemicals) for approximately 30 min. The LA was gently minced in the high-K^+ solution (KB solution) and the pieces were agitated to dissociate the cells. The cell suspension was stored at 4°C for later use.

Solutions

The composition of normal Tyrode's solution was (mmol/L): NaCl 136, KCl 5.4, $MgCl_2$ 0.5, $CaCl_2$ 1.8, NaH_2PO_4 0.33, HEPES 5.0, and glucose 5.5 (pH 7.4 with NaOH). The composition of KB solution was (mmol/L): KOH 70, KCl 30, L-glutamic acid 70, taurine 20, KH_2PO_4 10, $MgCl_2$ 1.0, glucose 1.0, EGTA 0.3, and HEPES 10 (pH 7.4 with KOH). The pipette solution was composed of (mmol/L): KOH 130, aspartic acid 80, Mg-ATP 5, KCl 20, HEPES 5.0, EGTA 5, and Na_2GTP 0.1 (pH 7.2 with aspartic acid). Cs-Tyrode's solution, which was prepared by replacing the KCl in normal Tyrode's solution with equimolar CsCl, was used for measuring whole-cell I_{CaL}. The Na^+/K^+-free pipette solution contained (mmol/L): CsOH 130, aspartic acid 80, TEA-Cl 20, Mg-ATP 5, HEPES 5, EGTA 10, and GTP-$Tris_2$ (pH 7.4 with aspartic acid).

Patch Clamp Experiments

The whole-cell voltage clamp method was used to record membrane currents. Patch pipettes were pulled with a microelectrode puller (model P-97; Sutter Instrument, Novato, CA, USA) and had a resistance of 2-5 MΩ when filled with internal solution. Membrane currents were recorded in the voltage-clamp mode using a patch-clamp amplifier (Axopatch B; Axon Instruments, Burlingame, CA, USA). The AP was elicited with a 0.5-ms depolarizing pulse at 0.5 Hz using a current-clamp mode. Experimental protocols, data acquisition, and storage were accomplished with CLAMPEX (Axon Instruments, Burlingame, CA, USA) and a personal computer.

Reverse Transcriptase Polymerase Chain Reaction (RT-PCR)

Total RNA was isolated from the LA and reverse transcription was performed using standard methods. For RT-PCR, 2.0 μl of template was used. Rat voltage-gated Ca^{2+} channel Cav1.2 subunit, atrial natriuretic factor (ANF), and brain natriuretic peptide (BNP) were then amplified using the following specific primers (5′ to 3′): Cav1.2 forward, ATGACAGACGCTATGGGC TATGAG; Cav1.2 reverse, GCATGC TCATGTTTC GGGGTTTGTC; ANF forward, ACCTGCTAGACC ACCTGGAGGAG; ANF reverse, CCTTGGCTGTTA TCTTCGGTACCG; BNP forward, CAGAACAA TCC ACGATGCAG; and BNP reverse, CGGTCTATCTTCT-GCCCAAA. Primers for β-actin were as follows: β-actin forward, GCTACAGCTTCACCACCACA; and β-actin reverse, AGGAAGGAAGGCTGGAAGAG. Comparative RT-PCR was performed under the same conditions with 25 cycles.

Statistical Analysis

All statistical data are presented as means±standard error. The non-paired t-test was used to compare physiological variations between the 2 groups. A difference of $p<0.05$ was considered statistically significant.

Results

Echocardiographic and Hemodynamic Measurements

TAC resulted in cardiac hypertrophy and heart failure at 8-10 weeks after surgery, as determined by echocardiographic recording and hemodynamic measurements. Echocardiographic study showed hypertrophy of the left ventricle with a significant increase in inter-ventricular septum wall thickness (1.78±0.05 mm, $n=14$ in the TAC group vs. 1.55±0.06 mm, n=17 in shams, $p<0.05$) and a significant decrease in EF (72.8±4.2%, $n=14$ in the TAC group vs. 89.5±3.3%, $n=17$ in shams, $p<0.05$) (Fig. 1A-C). Hemodynamics studies showed that systolic blood pressure between the bilateral carotid arteries was markedly different in the TAC group (Fig. 1D). TAC caused a pressure gradient of approximately 40 mmHg (41±5 mmHg, $n=14$) between the left and right carotid arteries.

Aortic Constriction Creates Cardiac Hypertrophy

The hearts were isolated at the 8th week post-operation. Fig. 2A shows representative heart views and a cross-section of hematoxylin/eosin staining at the level of the papillary muscle from TAC and sham-operated rats. We observed that the heart weight to body weight ratio was significantly larger in TAC rats than in shams (Fig. 2B) ($p<0.05$). Pressure-overloaded hypertrophy was observed in the left ventricle and LA. Masson-trichrome staining showed fibrotic change and an increase in cell size in the LA of TAC rats (Fig. 3A). The cross-sectional area of LA myocytes, measured from confocal microscopy imaging of tissue sections (Fig. 3A), was significantly larger in the TAC group than that of shams (143.4±5.36 μm^2, $n=100$ vs. 82.3±2.83 μm^2, $n=100$, $p<0.05$) (Fig. 3B). We also measured the cell membrane capacitance (C_m) in EPS (Fig. 3C). The C_m of LA cells was significantly larger in the TAC group (100.3±6.9 pF, $n=34$) than in the sham group (90.2±5.8 pF, $n=30$, $p<0.05$).

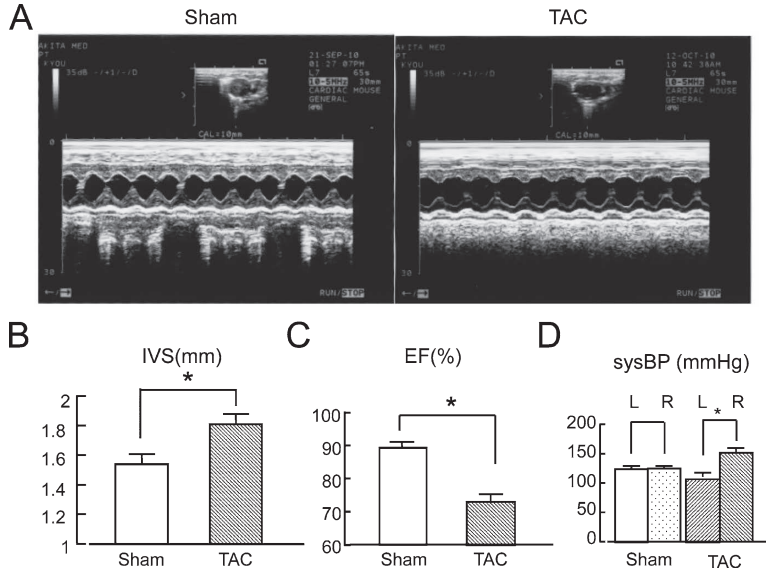

Fig. 1. In vivo echocardiographic assessment. A, Representative M-mode imaging of the left ventricular wall at a level beneath the mitral valve recorded from a TAC rat (left) and sham control rat (right) 8 weeks after surgery. B, Inter-ventricular septum wall thickness (IVS) was significantly increased in the TAC group compared with the sham group. C, The ejection fraction (EF) was significantly decreased in the TAC group compared with the control group. D, Systolic blood pressure of the right carotid artery was significantly higher than that of the left carotid artery in the TAC group. The statistical data are presented as the means ± SE. *$p<0.05$.

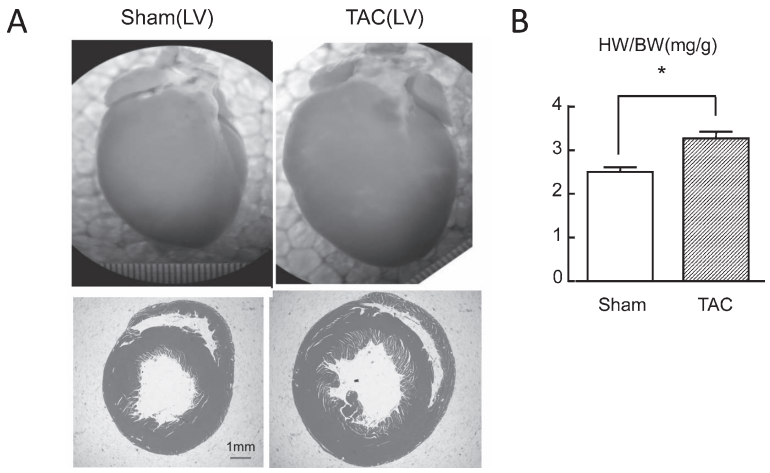

Fig. 2. Cardiac hypertrophy in response to pressure overload. A, Images of the whole heart and a hematoxylin/eosin stained cross-section of the left ventricle at 8 weeks after TAC or sham surgery. B, The heart weight to body weight ratio was significantly increased in the TAC group compared with the sham group. *$p<0.05$.

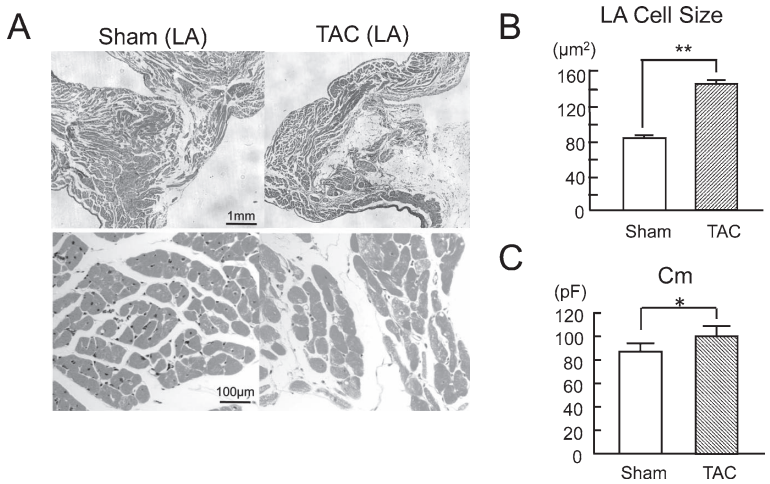

Fig. 3. Left atrial cell hypertrophy in TAC. A, Masson's trichrome staining and confocal microscopy imaging of left atrial tissue from TAC and sham rats. B, Cross-sectional area (μm^2) of left atrial cells from the TAC and sham groups as shown by confocal microscopy. C, Cell membrane capacitance (Cm) in left atrial myocytes. The statistical data are presented as the means ± SE. *$p<0.05$, **$p<0.01$.

EPS Findings and AF Induction

EPS studies showed that the AERP, measured by programmed atrial stimulation, was significantly shorter in the TAC group than that in shams at cycle lengths of 150, 120, and 100 ms ($p<0.05$, Fig. 4A). Fig. 4B shows a representative ECG record for AF induction. Atrial burst pacing was performed through the transvenous electrode catheter placed in the coronary sinus. Thirty-second burst pacing induced AF reproducibly in all rats of both groups and terminated spontaneously (Fig. 4B). However, AF inducibility was significantly higher in the TAC group compared with the sham group ($p<0.05$). AF was induced 19 times in 20 procedures (95%) in TAC

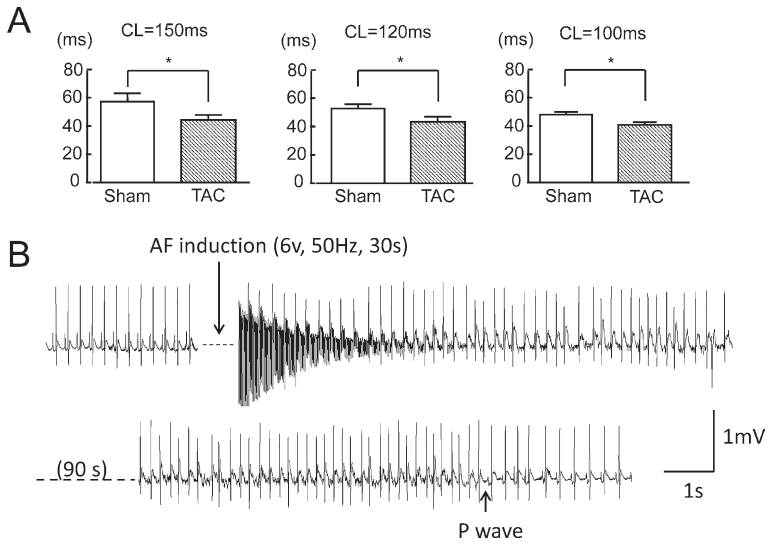

Fig. 4. Electrophysiological studies and AF induction in TAC. A, AERP measured during atrial-programmed stimulation was significantly shorter in the TAC group than in sham rats at cycle lengths of 150, 120, and 100 ms. (*$p<0.05$) B, Typical surface electrocardiogram (ECG) recordings during induced atrial fibrillation (AF). AF was reproducibly induced by 30-second atrial burst pacing from a transvenous electrode catheter via the cervical vein and spontaneously terminated to sinus rhythm.

rats and 15 times in 22 procedures (68.2%) in sham rats. The mean AF duration was significantly prolonged in TAC rats compared with that in shams (101.5±31.7 s, $n=19$ vs. 24.8±8.1 s, $n=15$, $p<0.01$). No severe complications, such as death or respiratory paralysis, were observed with this stimulation protocol in any rats.

APs of Atrial Myocytes

The APs were compared between atrial myocytes of TAC and sham-operated rats (Fig. 5A). APs in LA cells displayed a different configuration between TAC and sham rats. Repolarization of LA myocytes isolated from sham-operated rats was characterized by a rapid phase 1 repolarization followed by gradual repolarization, whereas repolarization of LA myocytes from TAC rats was more linear in form, with a less pronounced phase 1 (Fig. 5A). As a result, the AP duration (APD) of TAC myocytes was markedly shorter than that of sham myocytes (67.3±10.2 ms vs. 89.5±9.3 ms for APD_{90} ; 18.5±3.9 ms vs. 30.1±5.4 ms for APD_{50}, respectively, $p<0.05$), while the APD_{20} was not significantly different between the 2 groups (7.9±2.3 ms vs. 5.6±3.5 ms, Fig. 5C). No significant difference in the resting membrane potential was detected between TAC and sham rats. Interestingly, spontaneous automaticity was recorded in 10 LA myocytes of TAC rats, but not in sham-operated rats (Fig. 5B).

Electrophysiological Characteristics

Fig. 6A illustrates representative whole-cell current recordings of LA myocytes in normal Tyrode's solution obtained with 300-ms command pulses to potentials between −100 and +60 mV from a holding potential of −50 mV in both the TAC and sham groups. The pipette solution was a K^+-rich internal solution and the external solution was normal Tyrode's solution. The current-voltage (I-V) relationship showed that the currents at the end of the 300 ms pulses were markedly decreased in the TAC group compared with those in the sham group (Figure 6B) ($p<0.05$). The current densities at the test potential of +60 mV were 7.38±0.33 pA/pF ($n=7$) in the TAC group and 14.06±1.36 pA/pF ($n=6$) in the sham group.

The L-type Ca^{2+} channel current was recorded with

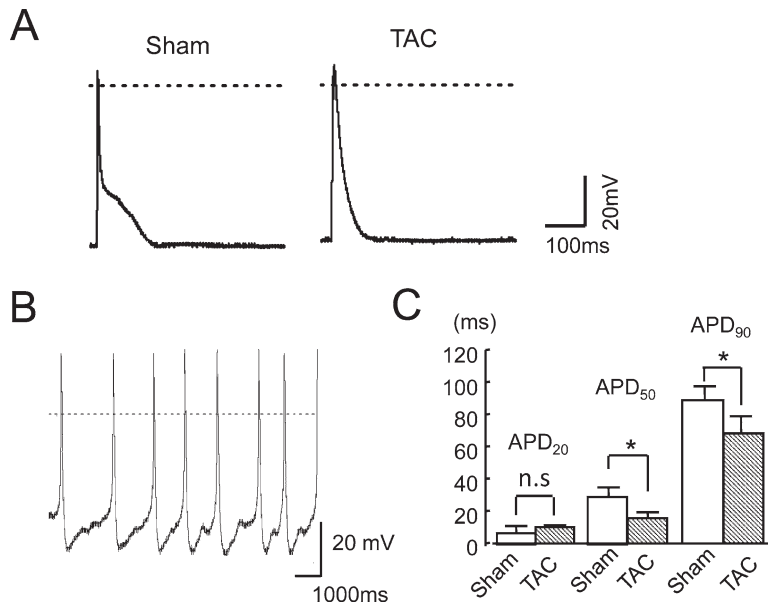

Fig. 5. Action potential and spontaneous automaticity of left atrial myocytes in rats. A, Representative action potentials of left atrial myocytes of the TAC and sham groups. B, Spontaneous automaticity of left atrial myocyte recorded in the TAC rat. C, Action potential duration (APD) values measured at 20%, 50%, and 90% repolarization in left atrial myocytes stimulated at 0.5 Hz are shown in the TAC ($n=10$) and sham ($n=9$) groups (*$p<0.05$).

patch-clamp technique. Myocytes were internally dialyzed with Cs^+-containing solution and perfused with Cs^+-Tyrode's solution. Fig. 6C shows representative families of current traces recorded by depolarization for 300 ms from a holding potential of −40 mV to various potentials between −70 and +60 mV in 10-mV increments. The I_{CaL} density was evaluated as a nisoldipine-sensitive (0.3 μM) current. Fig. 6D shows the I-V relation for 15 cells in the TAC group and 12 cells in the sham group. The I_{CaL} density was significantly smaller in the TAC group than that in the sham group (i.e., I_{CaL} density at +10 mV was −7.60±0.33 pA/pF in the TAC group and −9.15±0.30 pA/pF in the sham group, $p<0.05$).

RT-PCR Analysis of Calcium Channels

RT-PCR confirmed that Cav1.2 mRNA levels were decreased, and ANF and BNP mRNA levels were increased in LA myocardium of TAC rats compared with those of sham rats (Fig. 7A). The mRNA expression levels of Cav1.2 normalized to β-actin were significantly lower in the TAC group ($n=5$) than those in the sham group ($n=5$) (0.51±0.06 vs. 0.69±0.07, $p<0.05$; Fig. 7B). The mRNA expression levels of ANF and BNP normalized to β-actin were significantly higher in TAC rats ($n=5$) than those in sham rats ($n=5$) (ANF, 0.51±0.03 vs. 0.29±0.14, $p<0.05$; BNP, 0.62±0.11 vs. 0.21±0.10, $p<0.05$).

Discussion

In the present study, we showed that TAC efficiently induced left ventricular and atrial hypertrophy, associated with an increase in the inducibility of pacing-induced AF in rats. LA cell size was significantly larger in TAC rats than in sham-operated rats, as demonstrated by histological and electrophysiological experiments. Additionally, interstitial atrial fibrosis was observed to a greater degree in TAC rats than in sham rats. The AERP of the LA was significantly shorter and AF duration was significantly longer in TAC rats than in sham rats. Moreover, the I_{CaL} density of LA myocytes was decreased in TAC rats compared with sham rats, accompanied by a signifi-

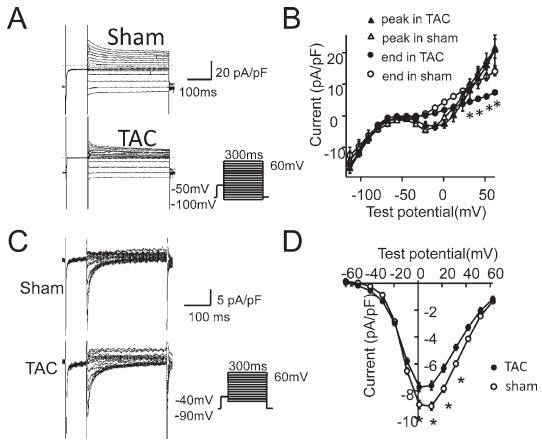

Fig. 6. Electrophysiological characterization of left atrial myocytes. A, Representative recordings of whole cell currents at 36°C in left atrial myocytes were obtained with the pulse protocol shown in the inset. B, Current-voltage (I-V) relationships of whole cell currents in left atrial myocytes isolated from the TAC (black) and sham (white) groups. C, Representative recordings of L-type Ca^{2+} channel current (I_{CaL}), evaluated as a nisoldipine sensitive current (0.3 μM). D, I-V relationship of I_{CaL} in left atrial myocytes from the TAC (black) and sham (white) groups. Data are presented as means ± SE. $^*p<0.05$ compared with sham myocytes.

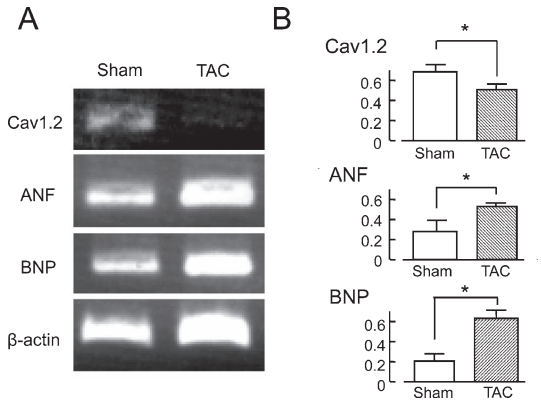

Fig. 7. Comparative RT-PCR analysis of left atrial cells from TAC rats. A, Expression levels of mRNA of Cav1.2, ANF, BNP, and β-actin. B, Relative density ratios to β-actin in TAC ($n=5$) and sham ($n=5$) rats. Data are means ± SE. $^*p<0.05$ vs. sham.

cant reduction in mRNA expression of the Cav1.2 subunit. All these findings indicate that TAC is a useful method for producing LA hypertrophy and the resulting alterations in electrophysiological properties of LA myocytes, and for investigating the mechanism of pressure overload-induced atrial remodeling.

Rat models of hypertrophy that lead to heart failure have been extensively used for studies involving cardiac function and related biochemical changes[11-15,16]. In the TAC model, heart failure develops in rats within 20-30 weeks after surgery[17], depending on the extent of the stenosis. This model, which closely mimics chronic hemodynamic stress or load observed in clinical heart failure, has proven useful for studying the progression to hypertrophy and transition to heart failure[17]. However, there is little information regarding atrial electric remodeling in an animal model of elevated afterload or hypertrophied atria. It has only been recently reported that partial stenosis of the ascending aorta causes atrial remodeling, which involves increased inducibility of AF and LA fibrosis[16]. In the present study, the TAC operation was successfully carried out under spontaneous breathing. The transverse aorta was accessed from the second left intercostal space via the mediastinal space, and a titanium clip was placed around the aortic arch. This technique has been proven a safe, simple, and effective technique for creating the model.

Our study demonstrated that the incidence and duration of pacing-induced AF were increased in the TAC group compared with those in the sham group, which is consistent with findings by Kim *et al.*[16]. They showed that, using rats with banding of the ascending aorta, hearts with elevated afterload were associated with marked LA hypertrophy and fibrosis. They also reported that vectorial conduction velocity was decreased and inhomogeneity in conduction was significantly enhanced without changes in the AERP. This finding is in contrast to the present study where the duration of the AERP and AP was significantly shortened in LA hypertrophy in TAC rats compared with shams. In the study by Kim *et al.*[16], LA hypertrophy was induced by banding of the ascending aorta, whereas TAC was used in the present study, where a significant pressure gradient was observed between the left and right common carotid arteries. Kim *et al.*[16] measured the AERP using excised

hearts, while we performed *in vivo* measurements of AERP. Furthermore, 3–4–week–old rats were used in the study by Kim *et al.*[16]. In our study, we used 8–week–old rats at the time of surgery. Therefore, the discrepancy between studies might be partially explained by the different experimental conditions. Alternatively, the severity of myocardial hypertrophy might have been different between the two studies. In our model, the EF was markedly reduced with a significant increase in the mRNA expression of ANF and BNP, which are known as important biomarkers in the diagnosis of heart failure. The inducibility and the duration of AF were much greater in the present study than those in the study by Kim *et al.*[16], where LA hypertrophy was achieved without heart failure. In addition, spontaneous automaticity was recorded in isolated LA myocytes of TAC rats (Figure 5B). Spontaneous automaticity is a potential cellular trigger for atrial arrhythmias associated with cardiac hypertrophy[18]. It has been also suggested that focal activity due to SA is one of the major mechanisms underlying atrial arrhythmias[19]. Therefore, atrial and ventricular hypertrophy, and resulting heart failure appeared to be more severe in the present study than those in the study by Kim *et al.*[16]. Nevertheless, all these findings are consistent with the view that atrial enlargement and hypertrophy are causal factors for the increased susceptibility to AF.

The present findings also indicate that shortening of the AERP and AP duration facilitates AF inducibility in hypertrophied atria. The reduced expression of I_{CaL} may have contributed to changes in APs, although remodeling of other ion channels, such as transient outward K^+ channels, also may have played a role. In the present study, I_{CaL} current density was significantly reduced in LA myocytes of TAC rats compared with sham–operated rats, accompanied by a decrease in Cav1.2 mRNA expression. Electrophysiological remodeling in left ventricular hypertrophy and heart failure has been extensively studied[20,21]. Although several clinical and experimental studies have indicated a decrease, no change, or even an increase in I_{CaL} density in CHF[8], it is generally agreed that mild hypertrophy does not appear to affect I_{CaL} abundance and function, whereas the development of severe hypertrophy is associated with a reduction in channel abundance and function[8,22,23]. In this respect, the reduction in I_{CaL} current density supports the notion that severe LA hypertrophy associated with heart failure was induced by the TAC procedure in the present study.

Rat atrial myocytes display a characteristic shape of APs. Early repolarization is followed by a low level of plateau, producing a notch at the beginning of the plateau. The change in AP configuration is dependent on the balance between inward and outward current systems. In addition to the contribution of I_{CaL} to the plateau, I_{to} is strongly involved in the early phase of repolarization[24]. It has been shown that chronic pacing–induced atrial remodeling involves a progressive attenuation in the rate of adaptation to the AERP, which is paralleled by a reduction of I_{CaL} and transient outward K^+ current. A marked decrease in the outward current observed in the present study (Fig. 6) might be consistent with this view.

In conclusion, the present study demonstrates that cardiac hypertrophy induced by the TAC operation results in arrhythmogenic remodeling of the LA, such as shortening of repolarization and down–regulation of I_{CaL} and possibly transient outward K^+ current, in a similar manner to chronic hemodynamic stress or load observed in clinical heart failure. These results indicate that left ventricular hypertrophy and heart failure cause increased hemodynamic load in the LA, resulting in structural and electrophysiological remodeling in LA myocytes.

Acknowledgments

We thank Dr. Shinichi Sato and Dr. Susumu Fujisawa in the Department of Cell Physiology, Akita University School of Medicine for their encouragement and technical assistance.

References

1) Heeringa, J., Van der Kuip, D.a.M., Hofman, A., *et al.* (2006) Prevalence, incidence and lifetime risk of atrial fibrillation : the Rotterdam study. *Eur. Heart J.*, **27**, 949–953.
2) Kirchhof, P., Lip, G.Y.H., Van Gelder, I.C., *et al.* (2012) Comprehensive risk reduction in patients with atrial fibrillation : emerging diagnostic and therapeutic

options — a report from the 3rd Atrial Fibrillation Competence NETwork/European Heart Rhythm Association consensus conference. *Europace,* **14**, 8-27.

3) Cleland, J.G.F., Coletta, A.P., Castiello, T. and Clark, A.L. (2011) Clinical trials update from the European Society of Cardiology Heart Failure meeting 2011 : TEHAF, WHICH, CARVIVA, and atrial fibrillation in GISSI-HF and EMPHASIS-HF. *Eur. J. Heart Fail.,* **13**, 1147-1151.

4) Juric, D., Yao, X., Thandapilly, S., *et al.* (2010) Defects in ryanodine receptor function are associated with systolic dysfunction in rats subjected to volume overload. *Exp. Physiol.,* **95**, 869-879.

5) Boixel, C., Gonzalez, W., Louedec, L.N. and Hatem, S. (2001) Mechanisms of L-Type Ca^{2+} Current Downregulation in Rat Atrial Myocytes During Heart Failure. *Circ Res*., **89**, 607-613.

6) Li, D., Melnyk, P., Feng, J., *et al.* (2000) Effects of Experimental Heart Failure on Atrial Cellular and Ionic Electrophysiology. *Circulation*, **101**, 2631-2638.

7) Le Grand, B.L., Hatem, S., Deroubaix, E., Couétil, J.P. and Coraboeuf, E. (1994) Depressed transient outward and calcium currents in dilated human atria. *Cardiovasc. Res.*, **28**, 548-556.

8) Mukherjee, R. and Spinale, F.G. (1998) L-type calcium channel abundance and function with cardiac hypertrophy and failure : a review. *J. Mol. Cell Cardiol*., **30**, 1899-1916.

9) Schrickel, J., Bielik, H., Yang, A., *et al.* (2002) Induction of atrial fibrillation in mice by rapid transesophageal atrial pacing. *Basic Res. Cardio*., **97**, 452-460.

10) Sugiyama, A., Takahara, A., Honsho, S., Nakamura, Y. and Hashimoto, K. (2005) Short Communication A Simple In Vivo Atrial Fibrillation Model of Rat Induced by Transesophageal Atrial Burst Pacing. *J. Pharmacol. Sic.,* **98**, 315-318.

11) Cantor, E.J., Babick, A.P., Vasanji, Z., Dhalla, N.S. and Netticadan, T. (2005) A comparative serial echocardiographic analysis of cardiac structure and function in rats subjected to pressure or volume overload. *J. Mol. Cell Cardiol.,* **38**, 777-786.

12) Biala, A., Martonen, E., Kaheinen, P., *et al.* (2010) Levosimendan improves cardiac function and survival in rats with angiotensin II-induced hypertensive heart failure. *Hypertension Res.,* **33**, 1004-1011.

13) Iwasaki, Y., Shi, Y., Benito, B., *et al.* (2012) Determinants of atrial fibrillation in an animal model of obesity and acute obstructive sleep apnea. *Heart Rhythm,* **9**, 1409-1416.

14) Koyama, T., Ono, K., Watanabe, H., *et al.* (2009) Molecular and electrical remodeling of L- and T-type Ca^{2+} channels in rat right atrium with monocrotaline-induced pulmonary hypertension. *Circ. J.,* **73**, 256-263.

15) Choisy, S.C.M., Arberry, L.a., Hancox, J.C. and James, A.F. (2007) Increased susceptibility to atrial tachyarrhythmia in spontaneously hypertensive rat hearts. *Hypertension,* **49**, 498-505.

16) Kim, S.J., Choisy, S.C.M., Barman, P., *et al.* (2011) Atrial remodeling and the substrate for atrial fibrillation in rat hearts with elevated afterload. *Circ. Arrhythm. Electrophysiol.,* **4**, 761-769.

17) Kagaya, Y., Hajjar, R.J., Gwathmey, J.K., Barry, W.H. and Lorell, B.H. (1996) Long-term angiotensin-converting enzyme inhibition with fosinopril improves depressed responsiveness to Ca^{2+} in myocytes from aortic-banded rats. *Circulation,* **94**, 2915-2922.

18) Guo, D., Young, L., Wu, Y., Belardinelli, L., Kowey, P.R. and Yan, G.X. (2010) Increased late sodium current in left atrial myocytes of rabbits with left ventricular hypertrophy : its role in the genesis of atrial arrhythmias. *Am. J. Physiol. Heart Circ. Physiol.,* **298**, H1375-1381.

19) Ciaccio, E.J., Ashikaga, H., Kaba, R.a., *et al.* (2007) Model of reentrant ventricular tachycardia based on infarct border zone geometry predicts reentrant circuit features as determined by activation mapping. *Heart Rhythm.,* **4**, 1034-1045.

20) Tomaselli, G.F. and Marbán, E. (1999) Electrophysiological remodeling in hypertrophy and heart failure. *Cardiovasc. Res.,* **42**, 270-283.

21) Jin, H., Lyon, A.R. and Akar, F.G. (2008) Arrhythmia mechanisms in the failing heart. *Pacing Clin. Electrophysiol.,* **31**, 1048-1056.

22) Workman, A.J., Kane, K.A. and Rankin, A.C. (2001) The contribution of ionic currents to changes in refractoriness of human atrial myocytes associated with chronic atrial fibrillation. *Cardiovasc. Res.,* **52**,

226-235.

23) Dinanian, S., Boixel, C., Juin, C., *et al.* (2008) Downregulation of the calcium current in human right atrial myocytes from patients in sinus rhythm but with a high risk of atrial fibrillation. *Eur. Heart J.*, **29**, 1190-1197.

24) Sah, R., Ramirez, R.J. and Backx, P.H. (2001) Modulation of Ca^{2+} Release in Cardiac Myocytes by Changes in Repolarization Rate : Role of Phase-1 Action Potential Repolarization in Excitation-Contraction Coupling. *Circ. Res.*, **90**, 165-173.